International Journal of Solids and Structures 47 (2010) 2591–2599

Contents lists available at ScienceDirect

International Journal of Solids and Structures

journal homepage: www.elsevier.com/locate/ijsolstr

Estimation of strengths in large annealed glass panels

I. Nurhuda [a,b,*], N.T.K. Lam [a], E.F. Gad [a,c], I. Calderone [d]

[a] Department of Civil and Environmental Engineering, The University of Melbourne, Parkville 3010, Australia
[b] Department of Civil Engineering, Diponegoro University, Semarang 50271, Indonesia
[c] Faculty of Engineering & Industrial Sciences, Swinburne University of Technology, Hawthorn 3122, Australia
[d] Calderone and Associates Pty Ltd. Consulting Engineers, Glen Waverley 3150, Australia

ARTICLE INFO

Article history:
Received 12 November 2009
Received in revised form 29 April 2010
Available online 24 May 2010

Keywords:
Glass strength
Large specimens
Weibull distribution
Monte Carlo
Flaw size distribution

ABSTRACT

A new model of the *Log-Normal* form for predicting the cumulative probabilistic distribution of strength in annealed glass panels is presented in this paper. The proposed model, which is supported by experimental evidences, shares certain features that are common with predictions by the *Weibull's* model. However, as the dimension of the panel is above a certain limit, the strength of glass as predicted by the new model is much less sensitive to any further increase in the panel dimension than strength predicted by the *Weibull's* model. This has important implications to the engineering design and risk assessments of glass facades in the future. The proposed alternative model was derived from results obtained from Monte Carlo simulations of non-interacting *Griffith* flaws based on principles of fracture mechanics. As interactions between flaws have been neglected in the analyses presented in the paper, the proposed model is intended to be applicable to glazing panels which contain widely spaced flaws. Results from physical experimentation in support of the simulation model have been presented in the paper.

1. Introduction

Glass Failure Prediction Model (GPFM) which underpins provisions in the ASTM standard (ASTM-E1300, 2007) for determining the load resistance of annealed glass panels subject to out-of-plane (mainly wind) pressure is defined by Eq. (1) which provides estimates for the probability of failure (F)

$$F = 1 - \exp\left\{-k \cdot \int [c(x,y) \cdot \sigma(q,x,y)]^m \cdot dA\right\} \quad (1)$$

where k and m are the dual *Weibull* parameters, $c(x,y)$ is the biaxial stress correction factor, and $\sigma(q,x,y)$ is the maximum principal stress which is expressed as a function of out-of-plane loading on the glass panel, the load duration and location within the panel.

Eq. (1) is based on the work of Beason (1998) and Beason and Morgan (1984) in which the *Weibull's* probability distribution function is adapted to the prediction of failure in glass. In the context of engineering mechanics, *Weibull's* model can be used to predict the strength of materials which are controlled by their weakest link. The *Weibull* distribution function has also been applied to many other facets of science and technology, including forecasts of extreme events and the quality control of manufactured products. Derivation of the *Weibull's* distribution relationship can be found in Weibull (1939) and Jayatilaka and Trustum (1977).

Weibull's expression for the cumulative probability distribution function has been simplified into Eq. (2) for conditions of pure uniaxial tensile stresses applied in one principal direction

$$F(\sigma) = 1 - \exp(-k \cdot \sigma^m \cdot A_{eff}) \quad (2)$$

where σ is the failure stress of the specimen, m and k are constants in the two-parameter version of the *Weibull* distribution function and A_{eff} is the effective area of the glass panel.

A common feature of Eqs. (1) and (2) is the use of the surface area of glass as a multiplier in the exponent of the *Weibull's* expression to represent the trend of decreasing strength in glass with increasing surface area. In situations of a panel subject to non-uniform stresses, analyses involve dividing the glass panel into elements. The contribution of each element to the cumulative probability of failure of the panel is taken into account by weighing the surface area of each element in accordance with the amount of stress to which the element is subjected. This functional form has been found to match experimental results through calibration of the *Weibull's* parameters. However, the influence of the surface area on the strength of the glass panel was not evident in the study by Calderone (2000) in which large panels measuring up to 2 m were tested.

The objectives of this paper are: (i) to examine the validity of this widely accepted feature in the *Weibull's* expressions (Eqs. (1) and (2)) in comparison with results obtained from both physical

* Corresponding author at: Department of Civil and Environmental Engineering, The University of Melbourne, Parkville 3010, Australia. Tel.: +61 3 83444709; fax: +61 3 8344 6215.
E-mail address: i.nurhuda@pgrad.unimelb.edu.au (I. Nurhuda).

0020-7683/$ - see front matter © 2010 Elsevier Ltd. All rights reserved.
doi:10.1016/j.ijsolstr.2010.05.015

and simulated experimentation (based on *Monte Carlo* simulations of non-interacting *Griffith* flaws in the panel); (ii) to investigate the statistical distribution of strength; and (iii) to study the effect of specimen size on the strength distribution of large glass panels.

Weibull expressions in Eqs. (1) and (2) are based on the assumption that *Weibull* parameters m and k are constant for specimens with the same material properties and glass surface conditions. Limitations of the *Weibull's* model are identified in Section 2 in which values of the *Weibull* parameters m and k obtained from physical experimentation are reviewed. An alternative simulation model for the probabilistic distribution of strength for panels subjected to two-way bending stresses is then developed in Section 3. The important issue of sample size is addressed in Section 4. The simulation model employs two main parameters namely flaw density and maximum flaw size. Both parameters have a direct physical meaning unlike the *Weibull's* parameters. The two parameters in the simulation model have been calibrated in order that the cumulative probability distribution (CPD) curves obtained from simulations corresponded with those derived from physical testings (Section 5). Given that the simulation model has been calibrated with test data, the calibrated parameters in the simulation model could be used for generating strength data for a wide range of panel dimensions including those that have not been sampled for physical experimentation. The simulated results are then used for modelling the probabilistic distribution of strength (Section 6) and size effects (Section 7).

2. Strength distribution of annealed glass panels from physical tests

The validity of Eqs. (1) and (2) which assume that the Weibull parameters m and k are constant is investigated in this section. To satisfy the ideal conditions of the Weibull expressions, new glass panels were used. Seventy-nine large glass panels of variable size were tested for this purpose. The specimens were divided into six different sets of dimensions, ranging from 2000 mm × 400 mm × 6 mm to 2000 mm × 2000 mm × 6 mm, as summarised in Table 1.

The specimens were simply supported on four sides and subjected to out-of-plane hydrostatic pressures. The boundary conditions of the panels resulted in two-way bending and biaxial stress states. The significant effects of the ratio of the principal stresses on the failure stress in glass have been studied by Bao and Steinbrech (1997) and Nurhuda et al. (2008). Thus, principal stresses recorded in the orthogonal directions have been transformed into equivalent uniaxial stress values (Nurhuda et al., 2008). Pressures were applied at different rates and results presented herein have been corrected to correspond with conditions of 3-s load duration based on the transformation relationships presented in Calderone (2000).

The cumulative probability distributions (CPD) of the corrected test results were obtained using Eq. (3)

$$F_i = \frac{i - 0.5}{N}, \quad i = 1 - N \tag{3}$$

where F_i is the cumulative probability of the ith ranked value in ascending order, and N is the number of specimens.

Table 1
Specimen size and number of specimens.

Size (mm)	Number of specimen
2000 × 400 × 6	15
2000 × 500 × 6	18
2000 × 670 × 6	15
2000 × 1335 × 6	10
2000 × 1600 × 6	11
2000 × 2000 × 6	10

The *Weibull* parameters were determined by calibration against the CPD of the ranked test results obtained for each batch of specimens of a given set of dimensions. The *Weibull* parameter m was identified by linear regression using Eq. (4) which was transformed from Eq. (2), by taking logarithms twice on both sides of the equation

$$Ln\{Ln[1/(1 - F(\sigma))]\} = m \cdot Ln\ \sigma + C \tag{4}$$

where C is a constant ($=Ln(k \cdot A_{eff})$) and $F(\sigma)$ can be calculated from the corrected (and ranked) test results based on Eq. (3).

The line of best-fit was constructed using the "least squares method" and m is the slope of the line of best-fit. The values of R^2 were calculated using Eq. (5)

$$R^2 = 1 - \left[\sum_{i=1}^{N}(d - x)^2\right] \Big/ \left[\sum_{i=1}^{N}(d - \bar{d})^2\right] \tag{5}$$

where d is the referenced value (from the sample); $\bar{d}$ is the sample mean, x is estimate by the line of best-fit, and N is sample size (number of specimens).

The value of parameter m so obtained from the calibration was used for calculating the effective area (A_{eff}) of the specimen of a given dimension using Eqs. (1) and (2). The value of parameter k was then calculated once the value of C has been found from calibration. This procedure for determining the value of m, C and k has been repeated for every batch of panel specimens of given dimensions.

The calculated *Weibull* parameters m and k are tabulated in Table 2 and compared with those from ASTM provision (ASTM-E1300, 2007) which stipulates constant values of k and m. The comparison shows very different values of the *Weibull* parameters m and k that have been obtained from calibrating with experimental test results involving panels of different dimensions. The displayed variability in the value of m and k (for glass panels obtained from the same source and manufacturing processes) contradicts with the notion of taking a single m value to represent "average conditions" as reported in the literature (ASTM-E1300, 2007; Hoshide et al., 1998). This observation reaffirms previous findings (Afferante et al., 2006; Kotrechko, 2003; Zwaag, 1989) that the *Weibull* parameter m is not a material constant.

Variability in the values of the m and k parameters obtained from calibration represents significant shortcomings in the use of the *Weibull's* model for generalising the probabilistic strength distribution behaviour of glass of variable dimensions. A more robust and reliable simulation model is presented in the rest of this paper. Development of the proposed model involved *Monte Carlo* simulations of individual flaws and bending stresses in the panel.

3. Simulation model

Brittle fracture in annealed glazing panels is always initiated from a *Griffith* flaw when the panel is subject to out-of-plane loading causing flexural tensile stresses on the glass surface. Usually, more than one flaw can be found in a panel. These flaws are

Table 2
Weibull parameters from calibration with test results in comparison with ASTM provision.

Panel size	Tests		ASTM	
	m	k (N^{-7} m^{12})	m	k (N^{-7} m^{12})
2000 mm × 400 mm	4.7	4.77×10^{-51}	7.0	2.86×10^{-53}
2000 mm × 500 mm	4.9	1.88×10^{-51}	7.0	2.86×10^{-53}
2000 mm × 670 mm	5.9	6.73×10^{-53}	7.0	2.86×10^{-53}
2000 mm × 1335 mm	8.5	3.51×10^{-57}	7.0	2.86×10^{-53}
2000 mm × 1600 mm	5.5	4.15×10^{-52}	7.0	2.86×10^{-53}
2000 mm × 2000 mm	3.3	8.39×10^{-49}	7.0	2.86×10^{-53}

randomly disposed within the panel and are of variable size but there is only one critical flaw that would potentially initiate fracture under ultimate load conditions. The larger flaws tend to have a higher probability of being the critical flaw. However, stress conditions surrounding the *Griffith* flaw can be a controlling factor as well. The initiation of fracture at a *Griffith* flaw is controlled by the *Stress Intensity* which can be used as the basis of accurately identifying the critical flaw in a panel for a given stress state (Griffith, 1920; Lawn, 1993).

The larger the size of the panel, the larger the number of flaws and the greater the chance of the panel having a larger flaw on its surface. Thus, the magnitude of tensile stress required to initiate facture is expected to decrease with increasing panel size. The objective of this section is to develop a simulation model based on the distribution of flaws for analysing the strength of glass. Whilst the simulation model presented herein is based on two-way bending, the model can be adapted to conditions of one-way bending or uniform bending.

3.1. The number and size of flaws and its distribution

The number of flaws in a specimen is dependent on the flaw density and surface area of the specimen. The probability that a specimen has n number of flaws can be defined in accordance with the Poisson distribution relationship of Eq. (6) (Gilvarry, 1961; Lemon, 1974).

$$f(n) = [(\rho \cdot A)^n / n!] \cdot [\exp(-\rho \cdot A)] \quad (6)$$

where ρ is the flaw density, n is the number of flaws, and A is the surface area.

According to fracture mechanics theory, a *Griffith* flaw can be characterised by two physical parameters: flaw shape and flaw size. Previous studies revealed that critical flaws found in broken glass plate specimens have the shape of a *half-penny crack*. The length of crack is identified as $2a$ and depth of crack as a (Krohn, 2002; Porter and Houlsby, 2001). Whilst the *half-penny crack* was adopted in the development of the proposed simulation model, the presented simulation techniques can be applied to any flaw shape by changing the value of the shape factor (Y) in the analysis.

One important step in the simulation is to determine the distribution of flaw size in the specimen as this would control the distribution of failure stress (Danzer, 2006; Danzer et al., 2001; Todinov, 2007). However, the distribution of flaw size in the specimen is difficult to measure by physical observations. Thus, the distribution of flaw size is normally derived from the distribution of fracture loads (Warren, 1995). Warren (1995) used this method to investigate the distribution of flaw size from specimens subjected to 3-point bending. Results show that the distribution of flaw size was right-skewed. However, Warren's method was based on the assumption that the cumulative probability distribution of strength followed the weakest link concept of Weibull.

This section examines different probability distribution functions for modelling the distribution of flaw size. This study differs from previous investigations in that the probabilistic distribution function of strength is not pre-determined. Instead, four different probabilistic distribution models have been used for simulating the size of individual flaws in the specimen as illustrated in Fig. 1(a)–(d): (i) *Uniform*, (ii) *Normal* (symmetrical) (iii) *Log-Normal* (right-skewed) and *Weibull* (left-skewed). The *abscissa* of the probability distribution functions (Fig. 1) is the normalised flaw size (r_j). With $r_j = 1$, the size of the flaw (a_j) is equal to the assumed maximum possible flaw size (a_{max}). This assumption of a maximum limit with the size of the critical flaw is reasonable for common manufacturing and installation processes of glass panels.

Each of the distribution functions considered herein has parameters characterising the shape of the distribution. Detailed descriptions of the considered distribution functions can be found in Ayyub and McCuen (1997). Since the normalised flaw size (r_j) was bounded in between the limits of 0 and 1, the statistical parameters of the functions were taken such that the cumulative probability at $r_j = 1$ was close to unity for every probabilistic distribution functions considered in this study. Parameters of the distribution functions used in the simulation has been summarised in Table 3.

3.2. Simulation techniques

Central to the simulation model is the identification of the critical flaw at which a crack could potentially initiate. There are six steps in the simulation procedure: (i) simulation of the number of *Griffith* flaw in a specimen, (ii) simulation of the size of each *Griffith* flaw, (iii) simulation of the disposition of each *Griffith* flaw

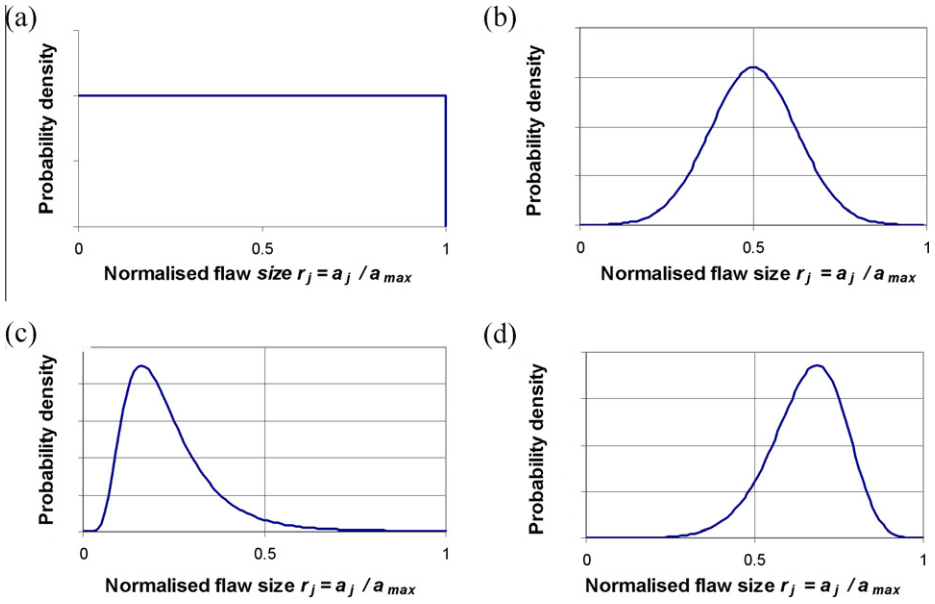

Fig. 1. Probability density functions for flaw size: (a) *Uniform* distribution; (b) *Normal* distribution; (c) *Log-Normal* distribution; (d) *Weibull* distribution.

Table 3
Statistical parameters for normalised flaw size (r) distribution.

Uniform	Normal	Log-Normal	Weibull
Max r: 1 Min r: 0	Mean r: 0.5 Std. Dev. r: 0.16	Mean $Ln(r)$: −3.14 Std. Dev. $Ln(r)$: 1	m: 7 k: 12.14

within the panel and identifying the level of stress at the simulated position, (iv) combining parameters determined in the previous steps for calculation of the strength ratio of each simulated flaw, (v) identifying the critical flaw which has the lowest calculated strength ratio, and (vi) calculation of the failure stress based on the critical flaw size. This six-step procedure is repeated for every simulated experiment. The strength values so obtained are ranked and the CPD values are determined using Eq. (3).

Probabilistic distribution of the number of *Griffith* flaws (n) in a specimen is defined by the Poisson relationship of Eq. (6). The number of *Griffith* flaws in each specimen was simulated in accordance with this relationship based on a random seed value which ranges between 0 and 1 (step i). After the number of flaws has been determined, the size of each individual flaw was determined in accordance with a chosen distribution function (Fig. 1) and a random seed value (step ii). Meanwhile, the x–y coordinates which define the position of each flaw in the panel are simulated. The λ_j parameter is then used to represent the level of stress, σ_j, at each simulated flaw position based on the stress contours (step iii). For example, consider a rectangular panel which is of size 2000 mm by 400 mm and 6 mm in thickness. The panel is simply supported on four sides (i.e., spanning two-ways) and is subject to uniform out-of-plane pressure (Calderone, 2000). Stresses in the glass panel were calculated using finite element analysis based on the elastic material properties. To reduce computational time, analyses were conducted on a quarter of the panel making use of symmetry about the orthogonal axes. The maximum principal stress contours identified for the quarter panels are shown in Fig. 2. The value of $\lambda_j = 1$ represents the relative level of stress for flaw no. j located at mid-span of the specimen (see Fig. 2). The strength ratio, S_j, of the simulated flaw is then calculated using the relationships of Eqs. (7a)–(7d) (step iv)

$$K_{IC} = \sigma_j Y\sqrt{(\pi a_j)} = \lambda_j \sigma_{max} Y\sqrt{(\pi a_j)} \tag{7a}$$

where K_{IC} is fracture toughness, Y is shape factor, λ_j is the normalised stress in the specimen at the position of the flaw, a_j is the size of the flaw, and $\sigma_{max}$is the maximum stress.

For the worst case of a flaw of assumed maximum possible size (i.e. $r_j = 1$; $a_j = a_{max}$) occurring at the maximum stress position (i.e. $\lambda_j = 1$; σ_j=σ_{max}), Eq. (7a) is re-written into Eq. (7b) in which the bending stress at mid-span is identified as the minimum stress σ_{min} required to cause failure

$$K_{IC} = \sigma_{min} Y\sqrt{\pi a_{max}} \tag{7b}$$

where a_{max} is the assumed maximum possible size of flaw.

Combining Eq. (7a) with (7b) gives Eqs. (7c) and (7d), the latter of which provides predictions for the strength ratio, S_j, for flaw no. j

$$\lambda_j \sigma_{max} Y\sqrt{(\pi a_j)} = \sigma_{min} Y\sqrt{(\pi a_{max})} \tag{7c}$$

$$\frac{1}{S_j} = \frac{\sigma_{min}}{\sigma_{max}} = \lambda_j \cdot \sqrt{\frac{a_n}{a_{max}}} = \lambda_j \cdot \sqrt{r_j} \tag{7d}$$

where S_j is the calculated strength ratio which varies between 1 and infinity for flaw no. j, r_j is the normalised size of the flaw.

The critical flaw is then obtained by sorting the $1/S_j$ values for identifying the most critical value (step v).

In a simplified procedure for obtaining a conservative estimate of the notional failure strength of glass, the critical flaw is assumed to be at the location of maximum stresses. Thus, the notional failure strength of glass (σ) can be calculated using Eq. (8)

$$\sigma = \frac{K_{IC}}{Y \cdot \sqrt{\pi \cdot r_j \cdot a_{max}}} \tag{8}$$

where K_{IC} is fracture toughness = 0.78 MPa m$^{1/2}$, Y is shape factor = 0.713 for half-penny shaped flaws (Fischer-Crips and Collins, 1995; Warren, 1995), r_j is the normalised size of the critical flaw, and $a_{max}$is the assumed maximum possible flaw size.

Eqs. (7)–(8) are based on the assumption that there is no interaction between flaws. In reality, however, two or more flaws that are very close to each other would alter the stress intensity at the crack tip (Afferante et al., 2006; Carpinteri et al., 2004; Jones et al., 1995). As a result, the strength of the glass pane could be lower than is estimated. To incorporate this phenomenon, the simulation model would need to be extended to include parameters defining distances between the simulated flaws. This is beyond the scope of the simulation model presented herein.

4. Effect of sample size (N)

A simulation technique for determining the strength distribution of glass has been presented in the previous section. However, the technique presented assumes that sample size (N) is sufficiently large to represent the actual distribution of strength in the entire population of glass materials. Thus, further investigations are required for studying the effects of sample size (N) on strength distribution, and in particular variability in strength within the sample. The aim is to find the required (minimum) value of N in a simulated experiment to achieve statistical significance. To achieve these objectives the CPD of failure stress from specimens of size 350 mm × 280 mm were simulated. The specimens were simply supported on all sides and subjected to out-of-plane distributed loading.

Simulations were based on a constant flaw density (ρ) of 10 flaws/m^2 and a maximum possible flaw size (a_{max}) of 278 μm. In each simulation the notional failure strength of the panel (σ_i) was calculated using Eq. (8) based on simulated values of r_j. With each sample, N number of simulations were undertaken and the simulated/calculated failure strengths were sorted and ranked in ascending order using Eq. (3) to determine the CPD curve for the sample.

CPD curves were constructed using this procedure for sample size of N = 15, 100, and 500. It is noted that the strength behaviour

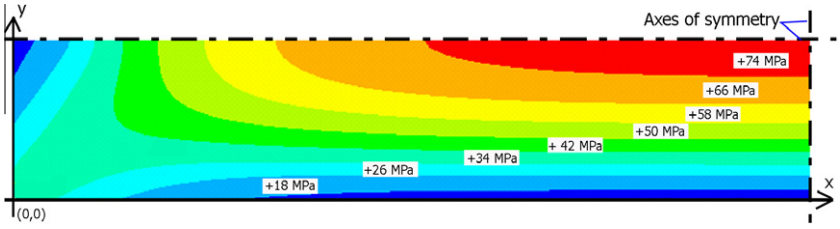

Fig. 2. Maximum principal stress in a specimen of size 2000 mm × 400 mm.

might vary significantly in between samples even if the panel dimension, source of manufacturing, age and conditions of handling and exposures have been kept the same. Recognising this, inter-sample variability was studied by repeating the sample simulations 25 times. The CPD curves obtained from each sample for $N = 15$ and 500 are plotted in Fig. 3(a) and (b) respectively. Each individual curve shown in Fig. 3(a)–(b) is the CPD representing a single sample of simulated specimens. Clearly, very high inter-sample variability is shown for samples of size $N = 15$. Thus, the simulated results for a single sample of this size in isolation do not have any statistical significance and hence the presented CPD could be misleading. More reliable estimates of the CPD can be obtained by increasing the value of N (i.e. number of specimens) of the sample as illustrated in Fig. 3(b) in comparison with Fig. 3(a).

Fig. 3(c) shows the clustering of the sample CPD curves about the "true" population CPD for N values of 15, 100 and 500. It appears that the mean of 25 samples is reasonably consistent with the "true CPD" irrespective of the sample size N as shown in Fig. 3(c). It is shown further in Fig. 3(d) that the two CPD curves representing the sample mean for $N = 100$ and 500 respectively are almost identical.

5. Verification of simulation model

In this section, the simulation model introduced in Section 3 is verified by calibrating the parameters of the model against results obtained from physical experimentation.

Three simulation parameters, namely the distribution function of flaw size $f(r)$, flaw density (ρ), and maximum critical flaw size (a_{max}) were calibrated. The calibrations were conducted in order that the simulated CPD curves matched with those obtained from physical experimentation.

The distribution of flaw size was investigated by analysing CPD curves that were derived from the four distribution models of flaw size: *Uniform*, *Normal*, *Log-Normal*, and *Weibull* distribution. Each of this models has the same maximum possible flaw size (a_{max}). The value of the flaw density was calibrated in order that the simulated CPD curves of strength best-fit the CPD curves obtained from physical experimentation. The calibrated flaw density values for each of the considered flaw size distribution functions are listed in Table 4.

Fig. 4(a) and (b) shows examples of CPD curves obtained from simulations and from physical experimentation of glass specimens of two different dimensions. The CPD curves for strength simulated in accordance with the right-skewed *Log-Normal* distribution of flaw size generally matched better with test results than the other considered distribution models (when $a_{max} = 278$ μm was specified). This is shown in Table 5 in which the values of R^2 characterising the goodness of fit are listed for each of the considered models for flaw size distribution. The *Weibull* distribution of flaw size is clearly not realistic given that the simulated CPD curves for strength based on this model were much more constrained than results obtained from physical experimentation. The same can be said of the *Normal* and *Uniform* distribution relationships for flaw size.

The distribution relationship for the normalised flaw size (r_j) is hence represented as follows:

$$f(r) = \left[1/\left(r\sqrt{2\pi}\right)\right] \exp[-0.5(Ln\, r + \pi)^2] \tag{9}$$

where r is the normalised flaw size.

Table 5 shows that five out of the six CPD curves obtained from simulations with the *Log-Normal* distribution of flaw size correlated better with physical test results than the other considered distribution functions (with values of R^2 exceeding 0.8). However, much lower values of R^2 have been observed with the larger glass panes for all the considered distribution functions. The reason for

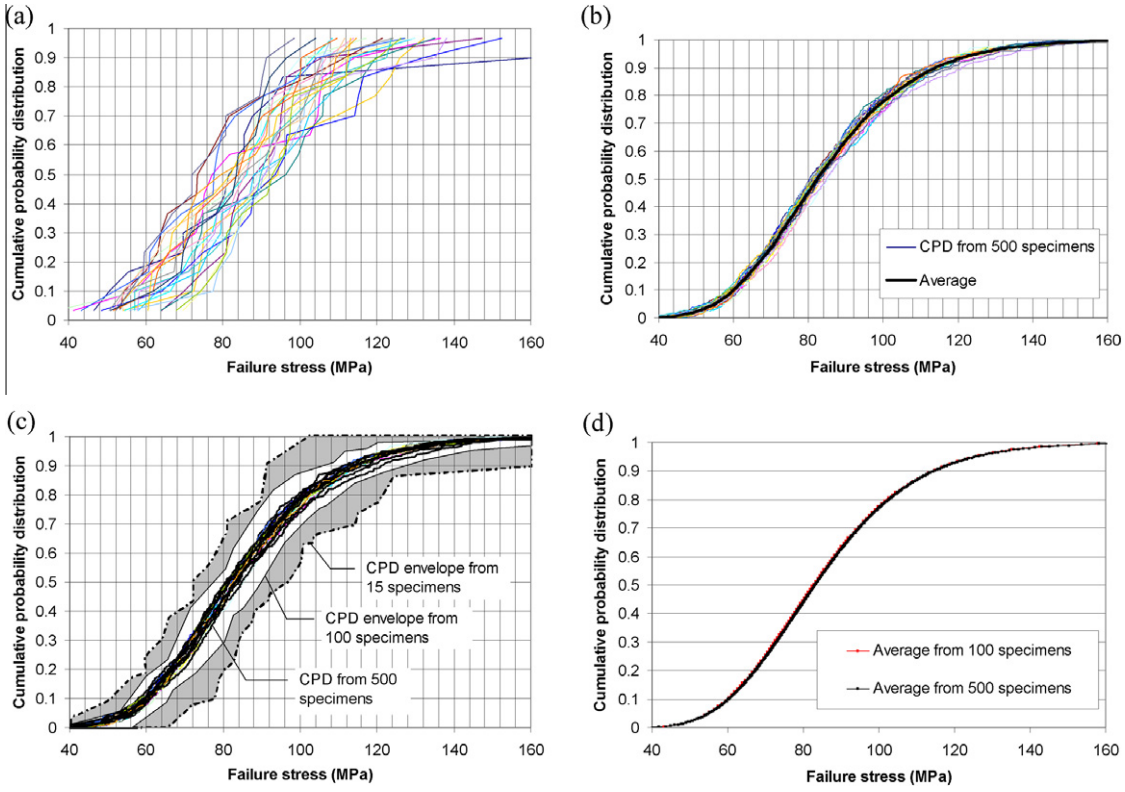

Fig. 3. CPD of notional failure strengths from simulated samples: (a) samples of $N = 15$ specimens; (b) samples of $N = 500$ specimens; (c) samples of $N = 15$, 100, and 500 specimens; (d) sample mean for $N = 100$ and 500 specimens.

Table 4
Flaw parameters (flaw density in flaws/m^2, and maximum flaw size (a_{max}) in μm).

Uniform	Normal	Log-Normal	Weibull
Flaw density: 2.5 a_{max}: 278	Flaw density: 1.0 a_{max}: 278	Flaw density: 10 a_{max}: 278	Flaw density: 0.5 a_{max}: 278

this is inconclusive in view of the limited data which is available. The authors do not rule out possible anomalies with flaw size distributions in large glass panes.

It has been shown in Section 4 that a small N value would result in highly variable CPD curves. Even better matches can be achieved by reducing the number of specimens in the simulated sample in order that the value of N for both the simulated and physical test samples are consistent (i.e. N = 10–18). However, inter-sample variability would be an issue for small N values.

6. Simulated strength of glass of variable dimensions

Experimental test programs have been conducted to investigate the probabilistic strength distribution behaviour of glass (Basu et al., 2009; Danzer et al., 2007; Doremus, 1983; Lu et al., 2002; Todinov, 2009). The investigations typically used specimens of limited dimensions. Given that large amount of data was required to provide a statistically meaningful estimate of the notional strength of glass, it would not be economical, nor practical, to conduct repetitive physical experimentation involving panels of the same dimensions as used in the building. Thus, the design of glass panels are often based on models that have been developed from the testing of specimens of much smaller dimensions. This extrapolation approach is shown herein to be heavily flawed.

The advantage of employing simulations is that the cost of experimental testings can be significantly reduced, especially when a wide range of specimen sizes are to be studied. However, physical experimentation would still be required for calibration and verification purposes. The specimens investigated in this section were assumed to have the same material properties and flaw conditions as those in the previous section. Thus, the calibrated *Log-Normal* distribution function as shown in Eq. (9) was used for modelling the distribution of flaw size.

Four different specimen dimensions ranging from 800 mm × 1000 mm to 2400 mm × 3000 mm were covered by the investigation. All specimens had the same aspect ratio of 1.25, simply supported on four sides, and subjected to out-of-plane uniform pressure. Such configuration of the glass panels results in almost identical stress contours as shown in Fig. 5. The strength distribution for each specimen size was analysed for N = 1000. Three statistical distribution functions: *Weibull*, *Normal*, and *Log-Normal*, were used for matching the CPD curves developed from the simulation model (Fig. 6).

Table 5
Coefficient of determination (R^2) showing goodness of fit with experimental tests results for different flaw size distribution functions used in simulations.

Panel size	Uniform	Normal	Log-Normal	Weibull
2000 mm × 400 mm	0.55	0.55	0.88	0.04
2000 mm × 500 mm	0.14	0.40	0.91	−0.31
2000 mm × 670 mm	0.24	0.39	0.93	−0.01
2000 mm × 1335 mm	−2.36	0.23	0.81	−0.23
2000 mm × 1600 mm	−0.33	0.57	0.81	0.71
2000 mm × 2000 mm	−0.55	0.18	0.30	0.21

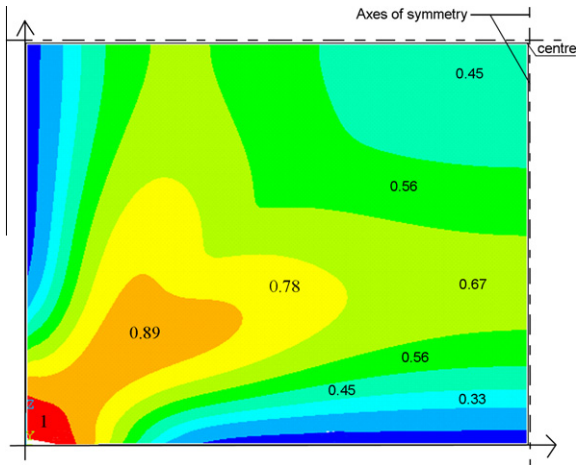

Fig. 5. Typical normalised maximum principal stress contour in specimens of size 800 mm × 1000 mm; 1200 mm × 1500 mm; 1600 mm × 2000 mm; and 2400 mm × 3000 mm.

The *goodness of fit* as shown by the value of the coefficient of determination (R^2) as defined by Eq. (5) are summarised in Table 6 which shows that the *Log-Normal* distribution function corresponds with the simulated strength data better than the *Normal* or *Weibull* distribution functions and particularly so at low probability of occurrences. This finding confirms earlier findings by the authors based on comparison with physical test results (Nurhuda et al., 2008).

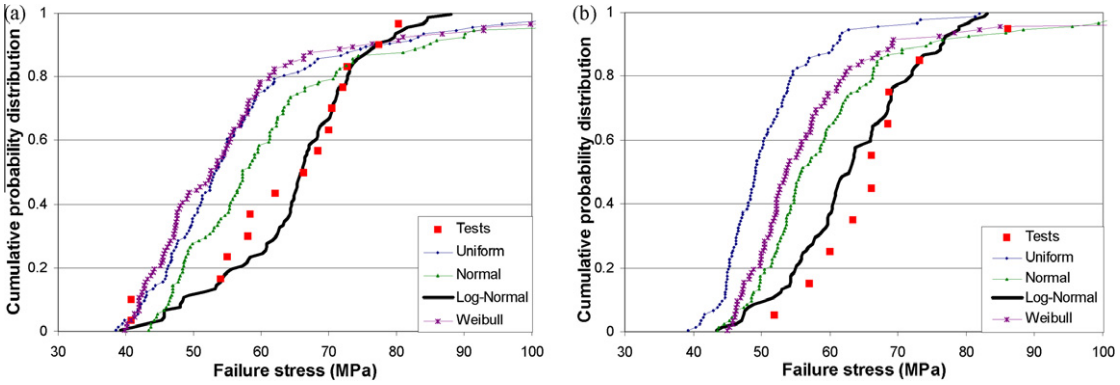

Fig. 4. Matching of simulated and calibrated CPD curves with experimental curves: (a) 2000 mm × 670 mm panels; (b) 2000 mm × 1335 mm panels.

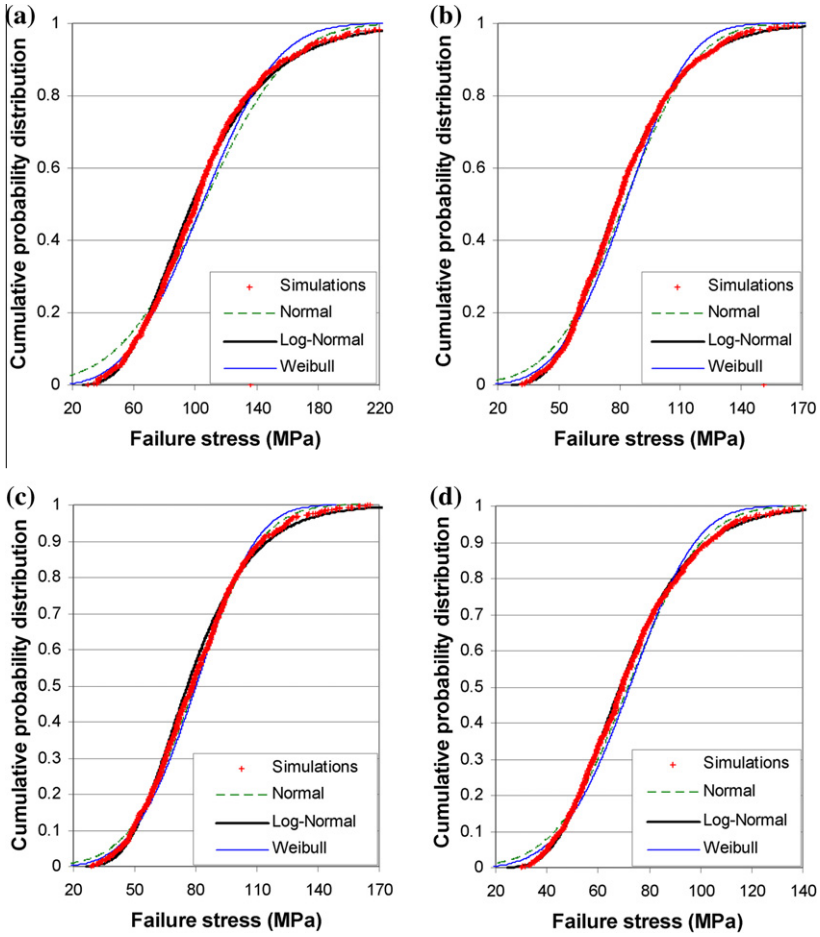

Fig. 6. Comparisons of CPD from simulated data and statistical functions: (a) 800 mm × 1000 mm panels; (b) 1200 mm × 1500 mm panels; (c) 1600 mm × 2000 mm panels; (d) 2400 mm × 3000 mm panels.

Table 6
Coefficient of determination (R^2) showing goodness of fit of different strength distribution functions with simulated test results.

Specimen size (mm)	Normal	Log-Normal	Weibull
1000 × 800	0.89	0.98	0.89
1500 × 1200	0.94	0.99	0.92
2000 × 1600	0.98	0.98	0.97
3000 × 2400	0.97	0.99	0.96

7. A proposed simplified representation of the size effects

The effect of size on the strength of glass was investigated numerically from glass panels of different sizes subjected to out-of-plane pressure. Four panel types of different dimensions have been analysed (Section 6). The aspect ratio of the specimens was kept at 1.25. The number of specimens for each panel size was taken to be 1000 in order that the sample CPD is a good approximation to the true population CPD.

The simulated CPD curves were matched by theoretical functions of the *Log-Normal* form (which had been found to match with the simulated data better than other considered theoretical functions as illustrated in Section 6). The *Log-Normal* probability distribution of strength ($f(\sigma)$) is represented by Eq. (10). The effect of specimen size on strength distribution behaviour is modelled by correlating the value of the *Log-Normal* parameters M and D with the physical surface area of the specimen as shown in Fig. 7

$$f(\sigma) = \left[1/\left(\sigma \cdot D \cdot \sqrt{2\pi}\right)\right] \cdot \exp[-(Ln\ \sigma - M)^2/(2 \cdot D^2)] \tag{10}$$

where D is the standard deviation of the natural logarithm of strengths and M is the mean of the natural logarithm of strengths.

It can be seen from Fig. 7 that the *Log-Normal* parameters M and D decrease as the surface area of the specimen increases. However, the rate of decrease in the value of M and D is clearly reduced with increasing panel size. The correlation of the *Log-Normal* parameters M and D with the panel surface area is represented by Eq. (11). In theory, the *Log-Normal* parameters M and D converge to the limit of 4.18 and 0.31 respectively for "infinitely large" glass panels

$$M = 4.18 \exp(0.08A^{-1.1}) \tag{11a}$$

$$D = 0.31 \exp(0.15A^{-1.1}) \tag{11b}$$

where A is the surface area of the specimen.

Eq. (11) is presented herein as the outcome of this study for providing a convenient and reliable means of estimating the strength of glass panels including those of large dimensions. Note that Eq. (11) would only be strictly valid for glass specimens with the same aspect ratio, load conditions, and minimum panel size as those considered in this study.

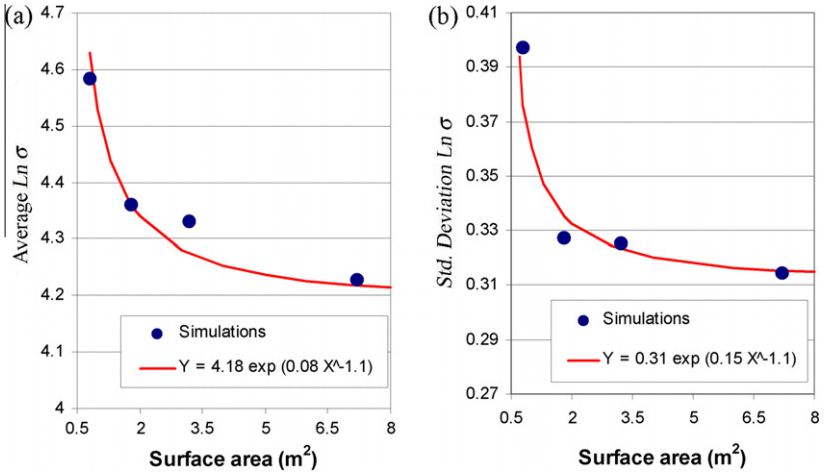

Fig. 7. Variation of Log-Normal parameters against actual area of specimen: (a) variation of the *Log-Normal* parameter *M*; (b) variation of the *Log-Normal* parameter *D*.

8. Conclusions

1. The calibrated values of the *Weibull* parameters are highly variable and unpredictable, and are dependent on many factors including panel dimensions, boundary and loading conditions, manufacturing and handling processes and age of exposure. Thus, the *Weibull* parameters m and k cannot be material constants.
2. The proposed (*Monte Carlo*) simulation model, which is based originally on principles of fracture mechanics and concept of *Griffith* flaws, is parameterised by flaw density and distribution of flaw size. Both of which has a direct physical meaning unlike the *Weibull* parameters. A flaw size distribution model of the *Log-Normal* form (Table 4 and Eq. (9)) has been found to translate into a CPD of strength that corresponds reasonably well with experimental results considered in the study.
3. With sample size of $N = 500$, inter-sample variability in the CPD of strength was effectively constrained and the sample CPD could be taken as the "true" (population) CPD. The mean of 25 samples of size $N = 100$ has also been shown to provide reasonable representation of the true CPD.
4. The CPD of strengths based on taking the sample mean of simulated results is best matched by theoretical relationships of the *Log-Normal* form. The behavioural trend of the CPD based on the simulated data has been studied.
5. A simplified *Log-Normal* representation of the size effects (Eqs. (10) and (11)) features a reduced rate in the decrease in the mean and standard deviation of $Ln(\sigma)$ with increasing panel size. The *Log-Normal* parameters characterising the probabilistic distribution of strengths converge as the dimension of the panel tends to "infinity".

References

Afferante, L., Ciavarella, M., Valenza, E., 2006. Is Weibull's modulus really a material constant? Example case with interacting collinear cracks. International Journal of Solids and Structures 43, 5147–5157.

ASTM-E1300, 2007. Standard practice for determining load resistance of glass in buildings. ASTM International, West Conshohocken.

Ayyub, B.M., McCuen, R.H., 1997. Probability, Statistics, and Reliability for Engineers. CRC Press, New York.

Bao, Y., Steinbrech, R.W., 1997. Strain criterion of fracture in brittle materials. Journal of Material Science Letters 16, 1533–1535.

Basu, B., Tiwari, D., Kundu, D., Prasad, R., 2009. Is Weibull distribution the most appropriate statistical strength distribution for brittle materials? Ceramics International 35, 237–246.

Beason, W.L., 1998. Basis for ASTM E1300 annealed glass thickness selection charts. Journal of Structural Engineering, ASCE 124, 215–221.

Beason, W.L., Morgan, J.R., 1984. Glass failure prediction model. Journal of Structural Engineering, ASCE 110, 197–212.

Calderone, I., 2000. The Equivalent Wind Loading for Window Glass Design. Ph.D. Thesis, Monash University.

Carpinteri, A., Brighenti, R., Vantadori, S., 2004. A numerical analysis on the interaction of twin coplanar flaws. Engineering Fracture Mechanics 71, 485–499.

Danzer, R., 2006. Some notes on the correlation between fracture and defect statistics: are Weibull statistics valid for very small specimens? Journal of the European Ceramic Society 26, 3043–3049.

Danzer, R., Lube, T., Supancic, P., 2001. Monte Carlo simulations of strength distributions of brittle materials-type of distribution, specimen and sample size. Zeitschrift fur Metallkunde 92, 773–783.

Danzer, R., Supancic, P., Pascual, J., Lube, T., 2007. Fracture statistics of ceramics-Weibull statistics and deviations from Weibull statistics. Engineering Fracture Mechanics 74, 2919–2932.

Doremus, R.H., 1983. Fracture statistics: a comparison of the Normal, Weibull, and Type I extreme value distribution. Journal of Applied Physics, American Institute of Physics 54, 193–198.

Fischer-Crips, A.C., Collins, R.E., 1995. Architectural glazing: design standards and failure models. Building and Environment 1, 29–40.

Gilvarry, J.J., 1961. Fracture of brittle solids: I. Distribution function for fragment size in single fracture (theoretical). Journal of Applied Physics 32, 391–399.

Griffith, A.A., 1920. The Phenomena of Rupture and Flow in Solids. Philosophical Transactions of the Royal Society of London A 221, 163–198.

Hoshide, T., Murano, J., Kusaba, R., 1998. Effect of specimen geometry on strength in engineering ceramics. Engineering Fracture Mechanics 59, 655–665.

Jayatilaka, A.D.S., Trustum, K., 1977. Statistical approach to brittle fracture. Journal of Material Science 12, 1426–1430.

Jones, R., Atluri, S.N., Pitt, S., Williams, J.F., 1995. Developments in the analysis of interacting cracks. Engineering Failure Analysis 2, 307–320.

Kotrechko, S.A., 2003. A local approach to brittle fracture analysis and its physical interpretation. Strength of Materials 35, 334–345.

Krohn, M.H., 2002. Biaxial flexure strength and dynamic fatigue of soda lime silicate float glass. Journal of American Ceramics Society 85, 1777–1781.

Lawn, B.R., 1993. Fracture of Brittle Solids. Cambridge University Press, New York.

Lemon, G.H., 1974. A problem in the distribution of maximum flaw length after inspection. Technometrics 16, 577–583.

Lu, C., Danzer, R., Fischer, F.D., 2002. Fracture statistics of brittle materials: Weibull or Normal distribution. Physical Review E 65, 1–4.

Nurhuda, I., Lam, N.T.K., Gad, E.F., 2008. The statistical distribution of the strength of glass. In: The 20th Australian Conference on The Mechanics of Structures and Materials, pp. 309–315.

Porter, M.I., Houlsby, G.T., 2001. Development of crack size and limit state design methods for edge-abraded glass members. The Structural Engineering 79, 29–35.

Todinov, M.T., 2007. An efficient algorithm for determining the risk of structural failure locally initiated by faults. Probabilistic Engineering Mechanics 2007, 12–21.

Todinov, M.T., 2009. Is Weibull distribution the correct model for predicting probability of failure initiated by non-interacting flaws? International Journal of Solids and Structures 46, 887–901.

Warren, P.D., 1995. Statistical determination of surface flaw distributions in brittle materials. Journal of the European Ceramic Society 15, 385–394.

Weibull, W., 1939. A Statistical Theory of The Strength of Materials. Generalstabens Litografiska Anstalts Förlag, Stockholm.

Zwaag, S.v.d., 1989. The concept of filament strength and the Weibull modulus. Journal of Testing and Evaluation 17, 292–298.

Ilham Nurhuda received his B.Eng in Civil Engineering from Diponegoro University, and MSc in Structural Engineering from Bandung Institute of Technology in Indonesia. He then worked as a structural engineer and an academic in Indonesia for 6 years. In 2007, he was awarded scholarships from Australian government and the University of Melbourne for pursuing a PhD degree. During his PhD candidature, he has done a series of numerical and physical experimentation to investigate the strength of glass panels subject to both static and impact loadings. His research interests are in the area of glass structures, numerical modelling and structural dynamics.

Nelson Lam, Reader in Civil Engineering at The University of Melbourne, is an internationally recognized expert in structural dynamics and engineering of structures for countering extreme loading. In the past 20 years, he has been researching and consulting widely in this field and has published some 200 technical articles. In recent years, he has extended his research interests into the impact resistant behaviour of glazing panels. His achievement in research and knowledge transfer was recognized by the award of the Chapman Medal (1999) and the Warren Medal (2006) by Engineers Australia.

Emad Gad obtained his BE (Hon) in Civil Engineering from Monash University, and PhD from the University of Melbourne. He is currently an Associate Professor at the University of Melbourne and Swinburne University of Technology, Australia. He has specific expertise in residential construction, structural dynamics and performance assessment of non-structural components. Emad has published over 100 refereed research papers and contributed to the development of national and international building standards.

Ignatius Calderone is a Director of Calderone and Associates Pty Ltd, Consulting Engineers based in Melbourne Australia. His expertise is in the areas of building façade design particularly with respect to all aspects of glass, including diagnostic investigations of glass failure, structural glass design and solar/thermal performance. Ignatius completed a Doctorate in the field of wind effects on glass in buildings. Ignatius has also presented several papers at international wind engineering and glass conferences and is involved with the preparation of the Australian and international glass standards.